Int. J. Electrochem. Sci., 16 **(2021)** Article ID: 210718, doi: 10.20964/2021.07.24

International Journal of
ELECTROCHEMICAL
SCIENCE
www.electrochemsci.org

Mn(III) and Fe(III) Porphyrin Complexes as Electrocatalysts for Hydrogen Evolution Reaction: A comparative study

Monirah H Alzabny, Raoudha Soury, Khalaf M Alenezi[*]

Department of Chemistry, College of Science, University of Ha′il, Ha′il, Kingdom of Saudi Arabia.
[*]E-mail: k.alenezi@uoh.edu.sa

Received: 11 March 2021 / *Accepted:* 20 April 2021 / *Published:* 31 May 2021

In the present work, we carried out comparative studies on electrochemical reduction of proton to molecular hydrogen, i.e. $2H^+ + 2e \rightarrow H_2$ using *meso*-tetrakis-(tetraphenyl)porphyrin iron(III) chloride [Fe(TPP)Cl] and *meso*-tetrakis(phenyl)porphyrin manganese(III) chloride [Mn(TPP)Cl] as electrocatalysts. Acetic acid (CH_3COOH) was used as the proton source. Results suggest that the reduction of CH_3COOH on the surface of vitreous carbon electrode (Ep = -1.8 V vs. Ag/AgCl in $[Bu_4N][BF_4]$-DMF) shifts to lower negative values in the presence of [Fe(TPP)Cl] and [Mn(TPP)Cl] (-1.6 and -1.3 V, respectively vs. Ag/AgCl). Analysis of peak current values indicated that [Fe(TPP)Cl] was more active (6 x) as compared to [Mn(TPP)Cl]. However, the [Mn(TPP)Cl]-catalyzed reduction process more swiftly (the potential is more positive than +30 mV).

Keywords: Electrocatalysis; hydrogen; iron, manganese complex, porphyrin

1. INTRODUCTION

Hydrogen Evolution Reaction (HER), which produces molecular hydrogen (H_2), is considered as one of the hot topics in the modern era [1-3]. H_2 is a promising candidate to tackle energy- and environment-related issues, a plethora of research has been devoted to the production of H_2 [4-7]. Production of hydrogen from a proton source using the electrochemical technique is a classical and intriguing technique [8-13]. The fast and inexpensive nature of the electrochemical reduction (ECR) method has attracted most researchers. However, the direct proton reduction at the electrode surface usually takes place at higher negative potential. An electrocatalyst is required to shift the reduction to fewer negative values. Generally, Pt(II), Mo(IV), W(IV), Pd(II)-based catalysts are employed for this purpose due to their high activity, but high cost and scarce nature often limit their practical application [14]. Despite seminal advances in this field, the design and development of economic catalysts remained a daunting task for chemists. Various nanostructured materials and organometallic complexes have been

designed and tested. Among many materials, porphyrin and metalloporphyrins have attracted significant interest from researchers. These N-containing macrocyclic compounds offer a wide variety of advantages, including easy functionalization, electroactive metal center, and wide-ranging solubility [6,7]. Following the seminal work on electrochemical hydrogen evolution from acidic media [15], several groups reported the ECR of protons as well as carbon dioxide using porphyrins [16] and metalloporphyrins [17,18]. Artero and co-workers [19] demonstrated that $[Co(bapbpy)Cl]^+$ (bapbpy: 6,6′-bis(2-aminopyridyl)-2,2′-bipyridine) catalyzes the electro-assisted H_2 evolution in DMF. They found that the catalytic pathways were significantly governed by the strength of the acid used as the proton source. Prior to this work, Moore and coworkers [20] demonstrated that binuclear Cu(II) porphyrins serve as active electrocatalysts for the HER. As per the authors, the reported catalyst possesses an extended macrocyclic structure leading to hydrogen production with near-unity Faradaic efficiency and maximum turnover frequency above 2000000 s^{-1}. Similarly, other studies based on porphyrinated Fe(I) [21], Rh(III) [22], Cu(II), Co(II) [23,24] have demonstrated the utility of this class of molecules for HER [25,26]. We herein report the electrochemical HER using two porphyrin complexes as electrocatalyst, i.e. meso-tetrakis-(tetraphenyl)porphyrin iron(III) chloride [Fe(TPP)Cl] and *meso*-tetrakis(phenyl)porphyrin manganese(III) chloride [Mn(TPP)Cl] (Chart 1). ECR was carried out at vitreous carbon electrode in the presence of acetic acid (CH_3COOH) as the proton source. Both [Fe(TPP)Cl] and [Mn(TPP)Cl] have been compared in terms of efficiency and activity.

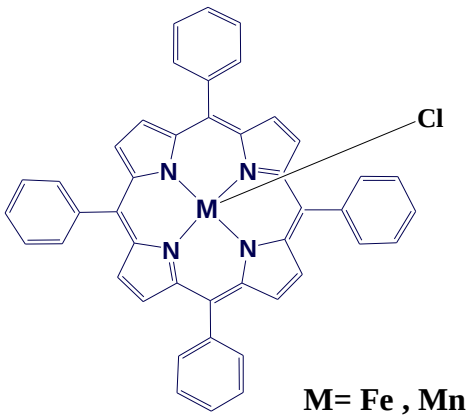

Chart 1. Chemical formula of [M(TPP)Cl], where M=Fe, Mn.

2. EXPERIMENTAL

[Fe(TPP)Cl], [Mn(TPP)Cl] and ligand of [(TPP)Cl] were synthesized and characterized according to previous report [27,28]. Acetic acid (CH_3COOH) and Dimethylformamide (DMF) were purchased from Sigma Aldrich. Cyclic voltammetry experiments were carried out using the potentiostat/galvanostat (Autolab PGSTAT 128N) with NOVA 1.10 software to record the electrochemical experiment results. A conventional three-electrode arrangement was employed, consisting of vitreous carbon working electrode (0.07 cm^2) and Ag^+ /AgCl reference electrode separated by a glass frits from a platinum wire auxiliary electrode (2 cm^2). The electrolysis cell containing 5 ml of

the electrolyte [NBu_4][BF_4] solution (0.2 M in DMF) was degassed with argon gas. 2 mM of catalyst [Fe(TPP)C] and [Mn(TPP)Cl] were added and stirred under N_2 in the electrochemical cell. The working electrode has a surface of 1 cm^2. The electrolysis in presence of [Fe(TPP)Cl], [Mn(TPP)Cl] were carried out at -1.6 and -1.3 V Ag+/AgCl respectively and the current was recorded during the course of electrolysis verses the time. The charge passed was recorded and the electrolysis was stopped when the current decayed after 45 minutes.

3. RESULTS AND DISCUSSION

3.1. Cyclic voltammetry of porphyrin complexes

Cyclic voltammetry study of the complexes ([Fe(TPP)Cl] and [Mn(TPP)Cl]) and ligand (TPPCl]) carried out at vitreous carbon in [NBu_4][BF_4] electrolyte solution (0.1 M in DMF). All potentials determined by cyclic voltammetry are given in Table 1 are quoted versus Ag|AgCl. In the presence of acid, [Fe(TPP)Cl] displays three successive reversible one-electron reduction processes [29]. Those steps, observed at potentials $E_{1/2}$= 0.15, -0.68, and -1.65 V versus Ag/AgCl, formally assigned to Fe(III)/Fe(II), Fe(II)/Fe(I) and Fe(I)/Fe(0) couples, respectively. On the other hand, [Mn(TPP)Cl] exhibit two reversible reductions peaks (-0.1 and -1.3 V versus Ag/AgCl) corresponding to Mn(III)/Mn(II) and Mn(II)/Mn(I), respectively.

Table 1. Potentials of reduction waves of Fe(TPP)Cl and Mn(TPP)Cl vs Ag|AgCl [NBu_4][BF_4]–DMF.

Complexes	**[Fe(TPP)Cl]**			**[Mn(TPP)Cl]**	
Reduction peak	Fe(III)/Fe(II)	Fe(II)/Fe(I)	Fe(I)/Fe(0)	Mn(III)/Mn(II)	Mn(II)/Mn(I)
E /V Ag^+/AgCl	0.15	-0.68	-1.65	- 0.1	-1.3

We also noted that the acetic acid reduces on the surface of the vitreous carbon electrode at Ep = -1.8 V vs. Ag/AgCl (Figure 1). This process (i.e., reduction) shifted to more positive potential values in the presence of Fe(TPP)Cl (200 mV) and Mn(TPP)Cl (450 mV) complexes.

The addition of the acid led to irreversible reduction waves in both the complexes, corresponding to Fe(I)/Fe(0) and Mn(II)/Mn(I). In addition to this, peak current also increases dramatically (Figure 2). In the presence of acid (CH_3COOH), CV of [Fe(TPP)Cl] showed a very large peak catalytic current at -1.65 V vs. Ag/AgCl, which we assigned to Fe(I)/Fe(0) couple. Interestingly, this value was ~ 11 times higher than one noted for [Fe(TPP)Cl] alone. The catalytic current tends towards a plateau at CH_3COOH ≥ 30 eq. These results are in accordance with the reported effect of [Fe(TPP)Cl] on the catalysis of electrochemical hydrogen evolution by at about -1.65 V *vs.* Ag/AgCl [15] using trifluoroacetic acid (TFA) as the proton source [30,31]. On the other hand, for [Mn(TPP)Cl], peak catalytic current was observed at -1.3 V *vs.* Ag/AgCl. Also, upon increasing the acid concentration, a second peak catalytic

step (3.5 times than peak in the absence of acid) was observed, which reached a maximum at about 20 equivalents of the acid.

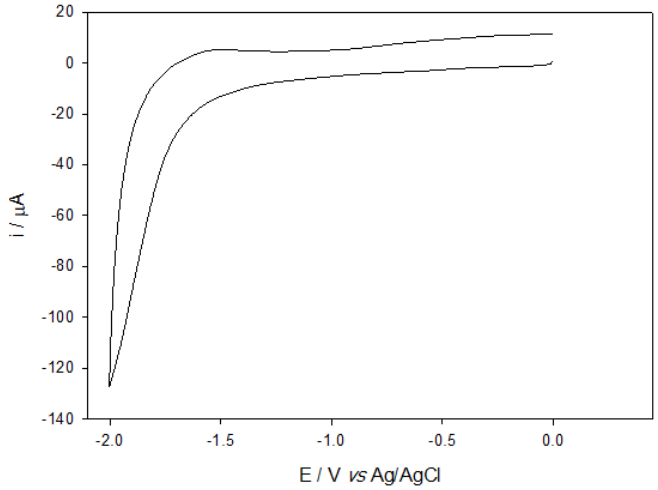

Figure 1. Cyclic voltammetry 2 mM CH_3COOH in $[Bu_4N][BF_4]$-DMF in the absence of catalyst. Scan rate 100 mVs^{-1} at vitreous carbon electrode *vs* Ag/AgCl.

Table 2. Potentials of reduction wave of (CH_3COOH) vs. Ag/AgCl $[NBu_4][BF_4]$ –DMF.

Reduction of CH_3COOH	**Potential/V *vs* Ag/AgCl**	**Shift**
Direct reduction	-1.8	0
In the presence of [Fe(TPP)Cl]	-1.65	180 mV
In the presence of [Mn(TPP)Cl]	-1.3	450 mV

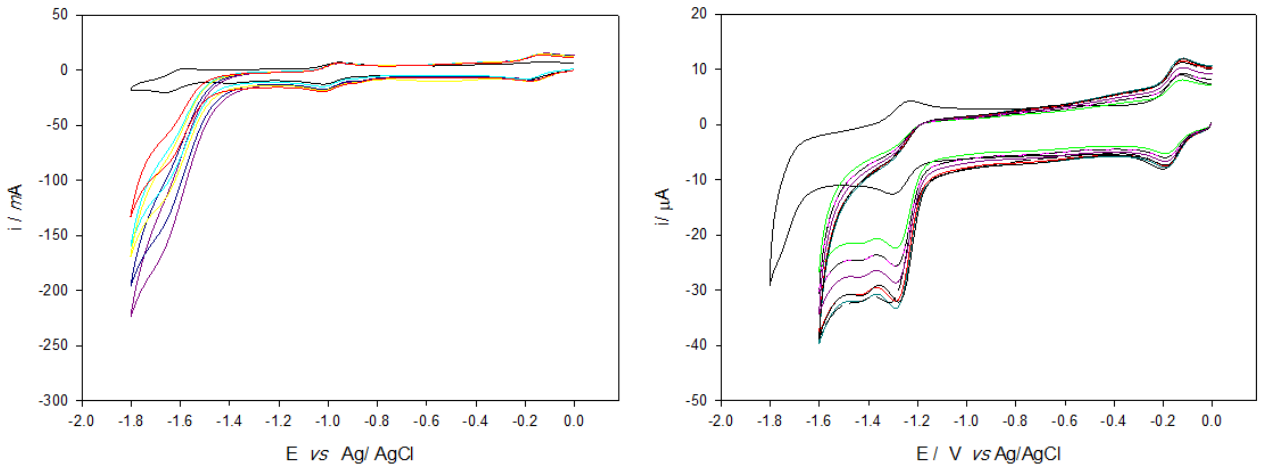

Figure 2. a) Cyclic voltammetry of 2 mM a) [Fe(TPP)Cl], b) [Mn(TPP)Cl] in $[Bu_4N][BF_4]$-DMF, scan rate 100 mVs^{-1} at a vitreous carbon electrode (0.07 cm^2) under N_2 in the presence of various concentrations of CH_3COOH.

3.2. Calculation of k_{cat}

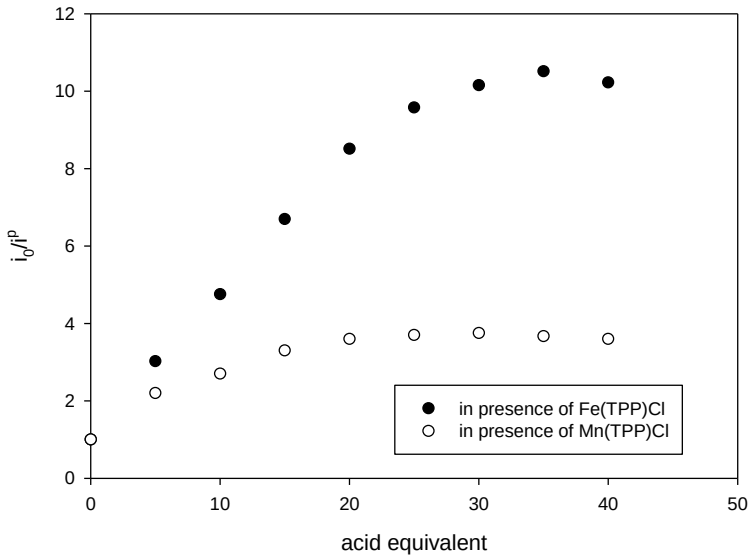

Figure 3. Comparison of the effect of the acid concentration on i_{cat}/i_0 ratio for the Fe(I)/Fe(0) Mn(I)/Mn(0) reduction wave on [Fe(TPP)Cl] , [Mn(TPP)Cl] respectively.

We also investigated the kinetics of electrocatalytic proton reduction. Figure 3 display the ratio of i_{cat}/i_0 at the electrode *versus* the concentration of acetic acid. The peak current, i_{cat}, is that measured at 100 mVs^{-1}, and i_0 is that for the peak current for Fe(I)/Fe(0) or Mn(I)/Mn(0) before the addition of acid at the same scan- rate. As it is clear from the figure, i_{cat}/i_0 become independent of the acid concentration at *ca* 30 eq. and 20 eq, for Fe(III) and Mn(I) complexes, respectively. The rate constant (k) at vitreous carbon was calculated using the eq. 1. and found to be 94.2 s^{-1} in the presence of [Fe(TPP)Cl] and 8.5 s^{-1}.

$k_{obs} = 0.1992(Fv/RTn^2)(icat/i_0)^2$ Eq. 1

where F, R and T are the Faraday constant, the gas constant and temperature, respectively; n is the number of electrons involved in the turnover.

The effects of Mn(TPP)Cl and Fe(TPP)Cl on HER are compared with the previously reported complexes (**Table 3**). As it is clear from the table, shifting of potential significantly dependent on the type of catalyst and proton source selected. For example, a positive shift in potential by 542 mV was reported when catalyst Co(TFPP) was used. Similarly, other iron complexes exhibited lower shift even tested using different sources of the protons.

Table 3. Comparing the effect of various complexes on HER

Complex	**Proton source**	**Potential of catalyst-free direct reduction (V)**	**Condition**	**Potential of reduction of acid in the presence of catalyst**	**Potential shifting**	**Ref.**
Mn(TPP)Cl	AcOH	-1.8 Ag/AgCl	$[NBu_4][BF_4]$ –DMF	-1.3 Ag/AgCl	450 mV	*Current work*
Fe(TPP)Cl	AcOH	-1.8 Ag/AgCl	$[NBu_4][BF_4]$–DMF	-1.60 Ag/AgCl	180 mV	*Current work*
Co(TFPP)	AcOH	-1.81 $Ag/AgNO_3$	$[NBu_4]ClO_4$–DMF	-1.45 V $Ag/AgNO_3$	542 mV	[32]
$[Fe_4S_4(SPh)_4]^{-2}$	Ltd	-1.36 Ag/AgCl	$[NBu_4][BF_4]$–Toluene	-0.87 V Ag/AgCl	490 mV	[33]
Fe(PFTPP)Cl	TEA	-1.6	$[NBu_4][BF_4]$–ACN	-1.3 V Ag/AgCl	300 mV	[34]
ACN = Acetonitrile, AcOH = Acetic acid, DMF = Dimethylformamide, LTD = 2,6-lutidine, TEA = Triethylamine						

3.3. Preparative–scale electrolysis

Preparative scale ECR using [Fe(TPP)Cl], [Mn(TPP)Cl] and H_2TPP was carried out in 0.1M $[Bu_4N][BF_4]$-DMF at room temperature in the presence of (CH_3COOH) on carbon electrode (1 cm^2) for 45 min.

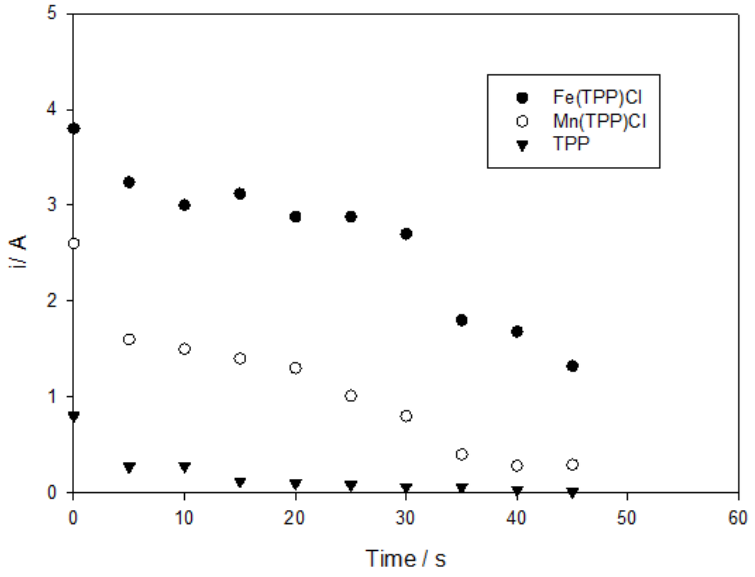

Figure 4. Current versus electrolysis time

The concentration of catalyst was 2 mM, and the solution contains 30 eq (CH_3COOH). Based on the cyclic voltammograms of [Fe(TPP)Cl], the applied potentials for electrolysis were set at -1.6 V

versus Ag/AgCl. As shown in figure 4, the current starts at 3.8 A, descends and stabilizes at 2.8 A (during 5-35 minutes), and then started to drop gradually until reaching 1.8 A. Under similar conditions and in the presence [Mn(TPP)Cl] at -1.3 V, the current started at 2.6 A, reaches a value of 1.6 A, then stabilized for 20 min, and then drops off dramatically. In the case of ligand, this value remained very low throughout the experiment.

Moreover, we also studied the charge passed vs. electrolysis time for 45 min. Summarily, we found that the charge increases over time. As compared to Mn(I) complex, the presence of Fe(III) doubled the charge value, whereas in the presence of the ligand, the charge value was very small.

3.4. Mechanism of HER

Based on previous HER studies, we have attempted to draw a possible mechanism of Mn(III) and Fe(III) complexes-mediated HER (Fig. 5 and 6). It has been reported that a metal complex could reduce the protons *via* five possible mechanisms, involving protonolysis and homolysis pathways [17]. It was suggested that H_2 evolution takes place through the formation of a formal $M^{(n-2)+}$ state which is obtained by the two-electron reduction of a metal catalyst [17]. These $2e^-$ reduction/protonolysis pathways have been well documented. In our case, [Mn(TPP)Cl] exhibit two reversible reductions peaks (-0.1 and -1.3 V *versus* Ag/AgCl, intermediate 2 & 3, Fig. 5). This is followed by oxidative protonation of 3 to form hydride intermediate 3. Finally, intermediate 3 undergoes protonolysis (react with a proton) to produce dihydrogen and initial metal complex.

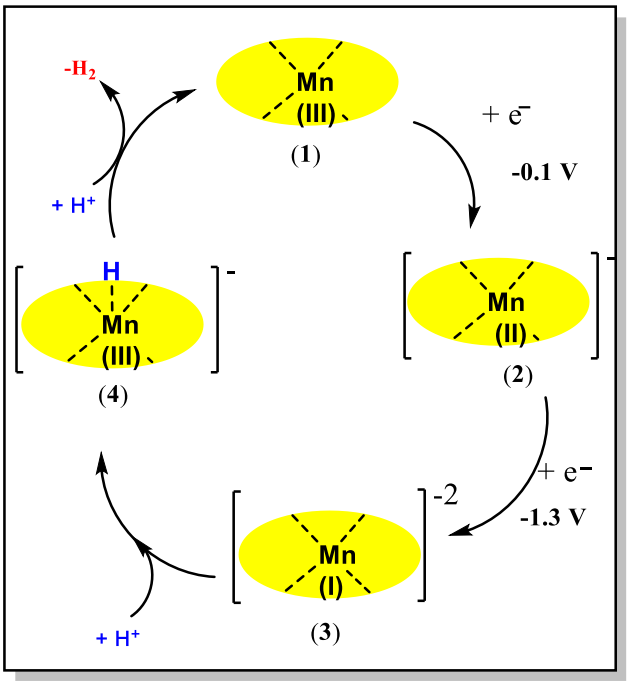

Figure 5. Possible mechanism of HER by Mn(III) complex.

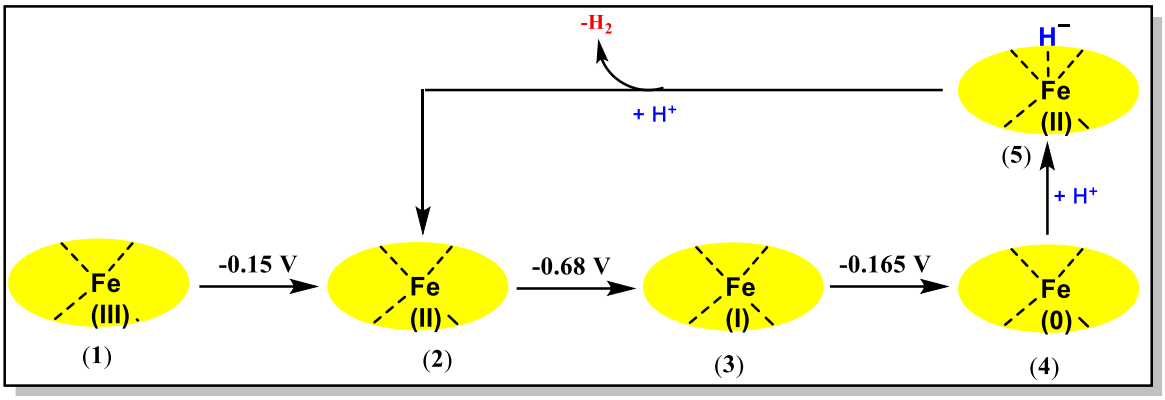

Figure 6. Possible mechanism of HER by Fe(III) complex.

On the other hand, we have noted that Fe(0) is the active species in the catalysis of HER (Fig. 2). This observation is in line with the previous works [35,36]. Based on this, we can say that Fe(0), obtained by the successive reduction {(Fe(III) → Fe(II) → Fe(I) → Fe(0)} form iron(II) hydride, which then reacts with a second acid molecule to evolve hydrogen (Fig. 6).

4. CONCLUSION

We have made a comparative study of Mn- and Fe-porphyrin complexes for hydrogen production using acetic acid as a proton source. As known, the direct reduction of (CH_3COOH) on the vitreous carbon electrode occurs at Ep = -1.8 V *vs.* Ag/AgCl. We found that Fe-porphyrin is an excellent electrocatalyst for converting the proton into hydrogen at carbon electrode in $[Bu_4N][BF_4]$-DMF electrolyte solution at room temperature at –1.60 V Ag/AgCl. On other hand, the hydrogen production can be shifted around 450 mV more positive potential in the presence of Mn-porphyrin. In addition, the rate constants (k^c_{cat}, room temperature) for the catalysis at carbon electrode in the presence of Fe- and Mn-porphyrin complexes are 94.2 S^{-1} and 8.5 S^{-1}, respectively (Figure 4).

References

1. R. E. Blankenship, D. M. Tiede, J. Barber, G. W. Brudvig, G. Fleming, M. Ghirardi, M. R. Gunner, W. Junge, D. M. Kramer and A. Melis, *Science*., 332 (2011) 805–809.
2. D. Gust, T. A. Moore and A. L. Moore, *Acc. Chem. Res*., 42 (2009) 1890–1898.
3. V. Balzani, A. Credi and M. Venturi, *Chem. Sus. Chem*., 1 (2008) 26–58.
4. J. L. Dempsey, B. S. Brunschwig, J. R. Winkler and H. B. Gray, *Acc. Chem. Res*., 42 (2009) 1995–2004.
5. M. L. Helm, M. P. Stewart, R. M. Bullock, M. R. Dubios and D. L. Dubios, *Science*, 333 (2011) 863–866.
6. R. M. Kellett and T. G. Spiro, *Inorg. Chem*., 24 (1985) 2373–2377.
7. R. M. Kellett and T. G. Spiro, *Inorg. Chem*., 24 (1985) 2378–2382.
8. S. Aresta, C. Nobile, V. Albano, E. Formi and M. Manassero, *Chem. Comm.*, 15 (1975) 636-637.
9. L. Bhugun, D. Lexa and J-M. Saveant, *J. Am. Chem. Soc.*, 118 (1996) 1769-1776.

10. E. E. Benson, C. P. Kubiak, A. J. Sathrum and J. M. Smieja, *Chem. Soc. Rev.*, 38 (2009) 89-99.
11. S. Nurhama and Y. Zhang, *Dalton Trans.*, 39 (2010) 3347-3357.
12. C. D. Windle and R. N. Perutz, *Coord. Chem. Rev.*, 256 (2012) 2562-2570.
13. M. Rosen, *J. Power Energy Eng.*, 3 (2015) 373-377.
14. A. Eftekhari, *Int. J. Hydrog. Energy*, 42 (2017) 1-25.
15. I. Bhugun, D. Lexa and J. Saveant, *J. Am. Chem. Soc.*, 118 (1996) 3982-3983.
16. J. C. Manton, D. Hidalgo, L. Frayne, M. P. Brandon, J. G. Vos and M. T. Pryce, *Int. J. Hydrog. Energy*, 43 (2018) 1-7.
17. W. Zhang and W. Lai and R. Cao, *Chem. Rev*., 117 (2017) 3717−3797.
18. B. B. Beyene and C. H. Hung, *Coord. Chem. Rev.*, 410 (2020) 213234.
19. N. Queyriaux, D. Sun, J. Fize, J. Pecaut, M. J. Field, M. Chavarot-Kerlidou and V. Artero, *J. Am. Chem. Soc.*, 142 (2020) 274-282.
20. D. Khusnutdinova, B. L. Wadsworth, M. Flores, A. M. Beiler, E. A. Reyes Cruz, Y. Zenkov and G. F. Moore, *ACS Catal*., 8 (2018) 9888–9898.
21. A. Rana, B. Mondal, P. Sen, S. Dey and A. Dey, *Inorg. Chem*., 56 (2017) 1783−1793.
22. V. Grass, D. Lexa and J. M. Savéant, *J. Am. Chem. Soc*., 119 (1997) 7526-7532.
23. B. B. Beyenea, A. W. Yibeltala and C.H. Hung, *Inorganica Chim. Acta*, 513 (2020) 119929.
24. C. Canales, A. F. Olea, L. Gidi, R. Arce and G. Ramírez, *Electrochim. Acta*, 258 (2017) 850-857.
25. M. Stiebritz and M. Reiher, *Inorg. Chem.*, 49 (2010) 5818-5823.
26. C. Tooley, S. Pazicni and E. Berda. *J. Polym. Chem.*, 6 (2015) 4279-4289.
27. L. A. Bottomley and K. M. Kadish, *Inorg. Chem*., 20 (1981) 1348.
28. Z. N. Zahran, J. Lee, S. S. Alguindigue, M. A. Khan and G. B. Richter-Addo, *Dalton Trans*., 1 (2004) 44-50.
29. K. Alenezi, *Int. J. Electrochem. Sci.*, 10 (2015) 4279-4289.
30. G. P. Connor, K. J. Mayer, C. S. Tribble and W. R. McNamara, *Inorg. Chem.*, 53 (2014) 5408-5410.
31. C. L. Hartley, R. J. DiRisio, T. Y. Chang and W. Zhang, W. R. McNamara, *Polyhedron*, 114 (2016) 133-137.
32. D. X. Zhang, H. Q. Yuan, H. H. Wang, A. Ali, W. H. Wen, A. N. Xie, S. Z. Zhan and H. Y. Liu, Transit. Met. Chem., 42 (2017) 773–782.
33. K. Alenezi. Electrochemical Transformation of Alkanes, Carbon Dioxide and Protons at Iron-Porphyrins and Iron-Sulfur Clusters (Doctoral dissertation, University of East Anglia), (2013).
34. K. Alenezi, *Int. J. Electrochem. Sci.*, 12 (2017) 812–818.
35. A. Rana, B. Mondal, P.Sen, S. Dey and A. Dey, *Inorg. Chem.*, 56 (2017) 1783-1793.
36. I. Bhugun, D. Lexa and J. Savéant, *J. Am. Chem. Soc.*, 118 (1996) 3982–3983.